

Transport coefficients from the 2PI effective action: weak coupling and large N analysis

Gert Aarts¹ and Jose M. Martínez Resco²

¹Department of Physics, University of Wales Swansea
Singleton Park, Swansea, SA2 8PP, United Kingdom

²Department of Physics & Astronomy, Brandon University
Brandon, Manitoba R7A 6A9, Canada

E-mail: g.aarts@swan.ac.uk, martinezrescoj@brandonu.ca

Abstract. The diagrammatic computation of transport coefficients in relativistic field theories is discussed. We show that the lowest nontrivial truncation of the two-particle irreducible (2PI) effective action correctly determines transport coefficients in a weak coupling or $1/N$ expansion at leading (logarithmic) order. In gauge theories, we verify gauge fixing independence and consistency with the Ward identity. These results support the applicability of 2PI effective action techniques to the study of nonequilibrium quantum-field dynamics.

1. Introduction

Motivated by the recent developments in heavy ion collisions as well as in inflationary cosmology, the dynamics of relativistic quantum fields out of equilibrium and their subsequent thermalization has been studied using various approximations: (inhomogeneous) mean-field theory (such as Hartree or leading-order large N approximations), classical approximations, kinetic theory, hard thermal loop effective theories, etc. One approach that has been particularly successful in the past few years [1] employs the 2PI effective action [2]. In order to better understand the hydrodynamic regime contained in the dynamics obtained from truncations of the 2PI effective action, it is interesting to see whether the 2PI framework gives reliable results for transport coefficients in the limit where a semi-analytical computation can be carried out, i.e. in a weak coupling or a large N expansion. Of course, the interest in transport coefficients is fueled as well by the physics of heavy ion collisions, where the presence of an appreciable shear viscosity would modify the ideal hydrodynamical description [3] of the aftermath of the collision [4]. Below we review how transport coefficients can be computed using the 2PI effective action as an organizational tool [5].

2. 2PI effective action

The 2PI effective action offers an approach to deal with the infinite hierarchy of correlation functions in field theory, based on a variational principle for one- and two-point functions. For a bosonic field theory, with vanishing mean field $\langle\phi\rangle = 0$, the effective action is written as [2]

$$\Gamma[G] = \frac{i}{2} \text{Tr} \ln G^{-1} + \frac{i}{2} \text{Tr } G_0^{-1}(G - G_0) + \Gamma_2[G], \quad (1)$$

where G_0^{-1} is the free inverse propagator. $\Gamma_2[G]$ contains all two-particle irreducible diagrams without external legs. For fermionic fields the $\frac{1}{2}$'s are replaced by -1 's. Since the 2PI effective action is formulated as a generating functional with external sources, similar to the 1PI effective action, higher order n -point functions are accessible as well. In particular, there is a four-point vertex function obeying a Bethe-Salpeter equation, which in momentum space reads

$$\Gamma^{(4)}(P, K) = \Lambda(P, K) + \frac{1}{2} \int_R \Lambda(P, R) G^2(R) \Gamma^{(4)}(R, K). \quad (2)$$

This equation sums ladder diagrams with a kernel Λ obtained from the second derivative of $\Gamma_2[G]$. It plays therefore a crucial role in the computation of transport coefficients [5] when these are determined by ladder diagrams, such as in scalar [6, 7] and large N_f gauge theories [8] to leading order and in weakly coupled gauge theories to leading logarithmic order [9, 10].

3. Loop expansion

As a first example we consider a scalar theory with a $g\phi^3 + \lambda\phi^4$ interaction. The 2PI contribution to the effective action up to three loops is shown in Fig. 1.

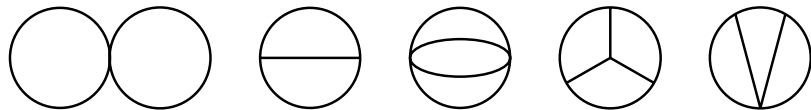


Figure 1. 2PI contribution to the effective action up to three loops in $g\phi^3 + \lambda\phi^4$ theory.

Differentiating this action twice yields the kernel that appears in the Bethe-Salpeter equation (see Fig. 2). This set of rungs indeed [5] contains all rungs that need to be considered to arrive at the correct result for the shear viscosity at leading order in the weak-coupling limit, found by Jeon some time ago [6] in a tour-de force calculation.

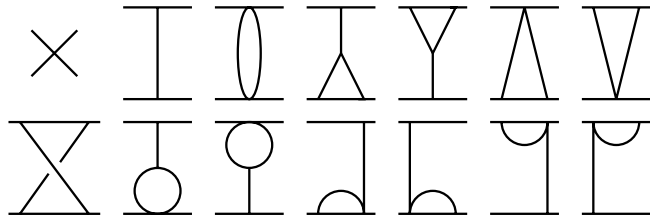


Figure 2. Kernel in the weakly coupled $g\phi^3 + \lambda\phi^4$ theory.

4. Large N expansion

Next we consider two theories in the large N limit: the $O(N)$ model [7] and large N_f QED/QCD [8]. The starting point is the 2PI contribution to the effective action in the $1/N$ expansion, shown in Fig. 3. In the $O(N)$ model there is a LO and a NLO contribution [11, 12, 13]. In large N_f QCD there is only a contribution at NLO. The chain of bubbles in the $O(N)$ model is indicated with the dashed line (see Fig. 4). In this formulation the scalar and gauge theory are conveniently similar. The results below are all generated from the graphs in Fig. 3, indicating the power of the 2PI formalism.

Extremizing the effective action yields the Schwinger-Dyson equations for the two-point functions, $S^{-1} = S_0^{-1} - \Sigma$, $D^{-1} = D_0^{-1} - \Pi$, where the resulting one-loop self energies still depend on the full propagators. In the computation of transport coefficients, the appearance of

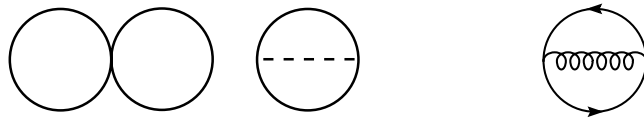


Figure 3. 2PI contribution to the effective action at LO and NLO in the large N limit in the $O(N)$ model (left) and at NLO in large N_f QCD (right). The dashed line in the $O(N)$ model sums the chain of bubbles, see Fig. 4.

$$\langle \rangle \cdots \langle \rangle = \times + \circlearrowleft \cdots \langle \rangle$$

Figure 4. Auxiliary correlator in the $O(N)$ model, summing the chain of bubbles.

full propagators is crucial for two reasons: to screen the so-called pinching poles [6], reflecting the dependence on the finite lifetime of quasiparticles due to collisions in the plasma, and to screen the divergences due to the exchange of offshell gauge bosons [14] (gauge theory only).

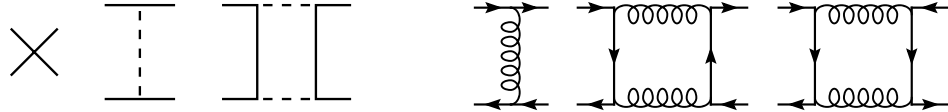


Figure 5. Kernels at LO and NLO in the large N limit in the $O(N)$ model (left) and at NLO in large N_f QCD (right).

Differentiating the effective action twice yields the rungs that appear in the Bethe-Salpeter equation. We find that some rungs contribute to the transport coefficients at leading order, whereas other rungs are subleading and can be neglected. In the large N expansion, power counting is fairly straightforward. Positive powers of N arise from two sources: closed loops of scalar or fermionic lines and scalar or fermionic propagators suffering from pinching poles (pinching poles are screened by the scalar or fermionic thermal width Γ_p and result in contributions $\sim 1/\Gamma_p \sim N$). Negative powers of N arise from the coupling constants, which are taken to scale as $1/N$ as is usually done in $1/N$ expansions. As a result we find the rungs given in Fig. 5.

To sum the ladder series, we use an effective three-point vertex \mathcal{D} . In terms of this vertex, the integral equations are shown in Figs. 6, 7. Again the propagators in these diagrams are

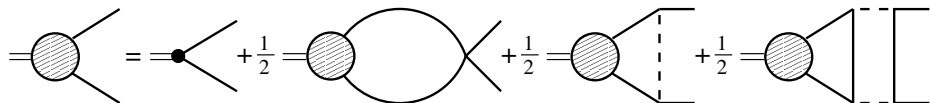


Figure 6. Integral equation for the effective vertex in the $O(N)$ model. The first closed loop on the RHS does not contribute, due to kinematical reasons.

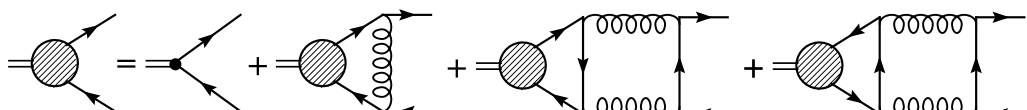


Figure 7. Integral equation for the effective vertex in large N_f QCD. In the case of the electrical conductivity, the last two contributions cancel, due to Furry's theorem.

still dressed. We consider these equations in the kinematical configuration special for transport coefficients: the energy entering on the left goes to zero, while the energy entering and leaving on the right is onshell. Transport coefficients are then extracted from the correlator obtained by closing the lines with an insertion of the appropriate current, indicated with the black dot.

The basic quantity we use to solve the integral equation is the ratio of the effective vertex $\mathcal{D}(p)$ and the thermal width $\Gamma_{\mathbf{p}}$, which we denote with χ . The shear viscosity in e.g. large N_f QCD then follows from a one-dimensional integral,

$$\eta = -\frac{d_F T_F}{C_F} \frac{2N_f}{15\pi^2} \int_0^\infty dp \frac{p^4}{\omega_{\mathbf{p}}} n'_F(\omega_{\mathbf{p}}) \chi(p), \quad (3)$$

after χ has been determined from the integral equation. In compact notation, the integral equation reads

$$\mathcal{F}(p)\chi(p) = \mathcal{S}(p) + \int_0^\infty dr \mathcal{H}(p, r)\chi(r), \quad (4)$$

where $\mathcal{F}(p) \propto \Gamma_{\mathbf{p}}$, $\mathcal{S}(p)$ is determined by the bare vertex, and $\mathcal{H} = \mathcal{H}_{\text{line}} + \mathcal{H}_{\text{box}}$ is determined by the rungs. This integral equation follows as the extremum condition from the functional

$$Q[\chi] = \int_0^\infty dp \left[\mathcal{S}(p)\chi(p) - \frac{1}{2}\mathcal{F}(p)\chi^2(p) + \frac{1}{2} \int_0^\infty dr \mathcal{H}(p, r)\chi(r)\chi(p) \right], \quad (5)$$

which allows for a variational treatment. The value at the extremum is immediately proportional to the shear viscosity.

5. Gauge fixing and Ward identity

In applications of 2PI effective action techniques to gauge theories, gauge fixing and Ward identities have to be considered [15]. It is therefore interesting to see where gauge fixing parameters appear and why they drop out in the calculation. We use the generalized Coulomb gauge such that the gauge field propagator,

$$D^{\mu\nu} = \Delta_T P_T^{\mu\nu} + \Delta_L g^{\mu 0} g^{\nu 0} + \xi \frac{P^\mu P^\nu}{p^4}, \quad (6)$$

consists of a transverse, a longitudinal, and a gauge fixing piece. The gauge fixing parameter ξ appears in three places:

- (i) thermal width. The imaginary part of the fermionic self energy is proportional to the discontinuity (spectral density) of the gauge boson propagator, i.e. to ρ_T , ρ_L . Since the gauge fixing part has no discontinuity, ξ drops out.
- (ii) line diagram. In the kinematical limit we consider also this contribution is proportional to the discontinuity of the gauge boson propagator and ξ drops out.
- (iii) box diagram. In the kinematical limit we consider *all* fermion lines are onshell and ξ drops out exactly.

One can also verify that the effective vertex in Fig. 7 and the fermion self energy are related via the Ward identity, again in the kinematical limit we consider. The analysis in this case is in fact easier than for the weakly coupled case [10], since the contribution to the thermal width arising from soft fermions in the latter is now subleading in the large N_f expansion [8].

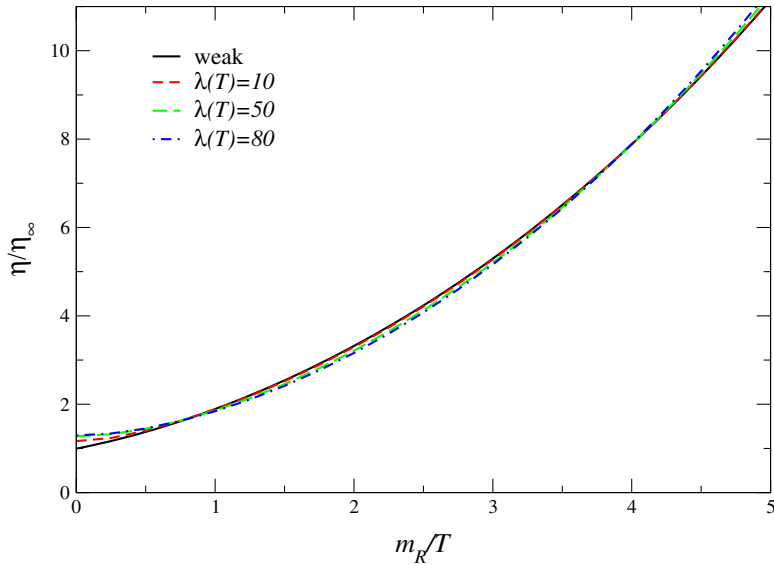


Figure 8. Shear viscosity in the $O(N)$ model vs. the renormalized mass at zero temperature for various values of the coupling constant $\lambda(\mu = T)$.

6. Variational solution

The integral equations are in general too complicated to be solved analytically. In the scalar case we found an approximate but surprisingly accurate solution for zero mass and vanishing coupling, which yields [7]

$$\eta_\infty = \frac{27648\zeta(5)}{\pi} \frac{N^3}{N+2} \frac{T^3}{\lambda^2} \approx 3041.9 \frac{3N^3}{N+2} \frac{T^3}{\lambda^2}. \quad (7)$$

In order to obtain the full N dependence and not just the leading order behavior $\sim N^2$ in the large N limit, we used the three-loop expansion of the 2PI effective action in the $O(N)$ model. The result for the numerical prefactor is very close to the full results obtained numerically by Jeon [6] (3040) and Arnold, Moore and Yaffe [16] (3033.5) for $N = 1$.

For arbitrary values of the mass and coupling constant (limited by the presence of the Landau pole), we solve the integral equations variationally. The function χ is expanded in a set of trial functions and the remaining integrals are performed numerically. The shear viscosity in the $O(N)$ model, normalized with the analytical result (7) in the large N limit, is shown in Fig. 8 as a function of renormalized mass at zero temperature for various values of the running coupling constant (the result is renormalization group independent). We find that the shear viscosity increases monotonically with increasing mass. This behavior was also found by Jeon [6] for $N = 1$. Interestingly, we find surprisingly little dependence (apart from that contained in η_∞) on the coupling constant, for all values allowed by the Landau pole.

For large N_f QCD the shear viscosity is shown as a function of fermion mass in Fig. 9, again for several values of the effective coupling constant g_{eff} ($g_{\text{eff}}^2 = T_F g^2 N_f$). The viscosity is normalized with $\eta_0 = d_F/(T_F C_F) \times T^3/g^4$. In this case we observe a nontrivial dependence on the mass. After a slight increase, we find that the viscosity decreases with increasing mass. This behavior is caused by longitudinal gauge bosons below the lightcone and can be understood using elementary kinetic considerations.

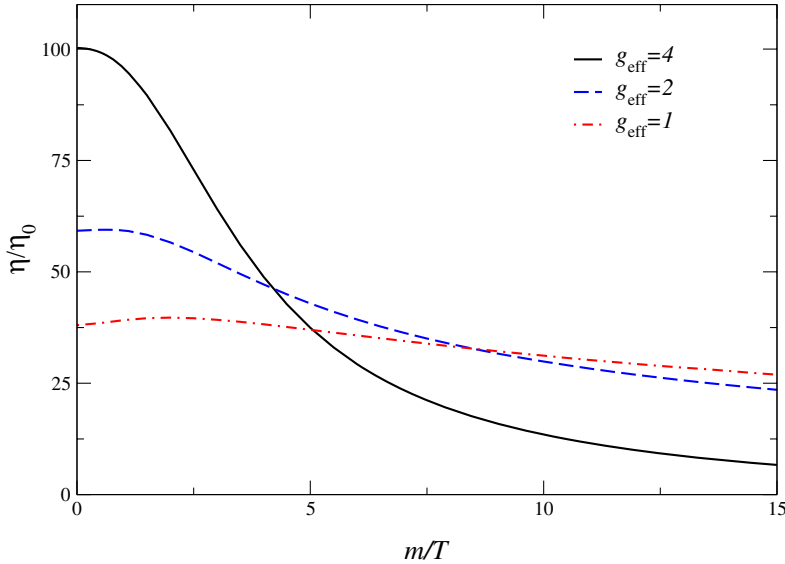


Figure 9. Shear viscosity in large N_f QCD vs. the fermion mass for various values of the effective coupling constant $g_{\text{eff}}(\mu = \pi \exp^{-\gamma_E} T)$.

7. Conclusion

The diagrammatic calculation of transport coefficients in a variety of relativistic field theories is well organized when the 2PI effective action is used: all necessary summations are generated by a few diagrams in the effective action. This diagrammatic understanding of transport coefficients provides necessary insight in the dynamics of quantum fields out of equilibrium. Our results provide further support for the applicability of truncations of the 2PI effective action to nonequilibrium QFT.

Acknowledgments

G.A. is supported by a PPARC Advanced Fellowship. J.M.M.R. was supported in part by the Spanish Science Ministry (Grant FPA 2002-02037) and the University of the Basque Country (Grant UPV00172.310-14497/2002).

References

- [1] For a recent review, see e.g. Berges J 2005 *AIP Conf. Proc.* **739** 3 (*Preprint* hep-ph/0409233)
- [2] Cornwall J M, Jackiw R and Tomboulis E 1974 *Phys. Rev. D* **10** 2428; Luttinger J M and Ward J C 1960 *Phys. Rev.* **118** 1417; Baym G (1962) *Phys. Rev.* **127** 1391
- [3] See e.g. Kolb P F and Heinz U (2003) in *Quark gluon plasma* 3 pp. 634-714, ed Hwa R C et al [nucl-th/0305084]
- [4] Teaney D 2003 *Phys. Rev. C* **68** 034913
- [5] Aarts G and Martínez Resco J M 2003 *Phys. Rev. D* **68** 085009 (*Preprint* hep-ph/0303216)
- [6] Jeon S 1995 *Phys. Rev. D* **52** 3591 (*Preprint* hep-ph/9409250)
- [7] Aarts G and Martínez Resco J M 2004 *JHEP* **0402** 061 (*Preprint* hep-ph/0402192)
- [8] Aarts G and Martínez Resco J M 2005 *JHEP* **0503** 074 (*Preprint* hep-ph/0503161)
- [9] Valle Basagoiti M A 2002 *Phys. Rev. D* **66** 045005 (*Preprint* hep-ph/0204334)
- [10] Aarts G and Martínez Resco J M 2002 *JHEP* **0211** 022 (*Preprint* hep-ph/0209048)
- [11] Berges J 2002 *Nucl. Phys. A* **699** 847 (*Preprint* hep-ph/0105311)
- [12] Aarts G and Berges J 2002 *Phys. Rev. Lett.* **88** 041603 (*Preprint* hep-ph/0107129)
- [13] Aarts G, Ahrensmeier D, Baier R, Berges J and Serreau J 2002 *Phys. Rev. D* **66** 045008 (*Preprint* hep-ph/0201308)
- [14] Baym G, Monien H, Pethick C J and Ravenhall D G 1990 *Phys. Rev. Lett.* **64** 1867
- [15] Arrizabalaga A and Smit J 2002 *Phys. Rev. D* **66** 065014 (*Preprint* hep-ph/0207044)
- [16] Arnold P, Moore G D and Yaffe L G 2000 *JHEP* **0011** 001 (*Preprint* hep-ph/0010177)